Drug Design, Development and Therapy

Dovepress
open access to scientific and medical research

Open Access Full Text Article

ORIGINAL RESEARCH

# Evaluation of Different Surface Coating Agents for Selenium Nanoparticles: Enhanced Anti-Inflammatory Activity and Drug Loading Capacity

Aml I Mekkawy[1], M Fathy[2], Hebatallah B Mohamed[3]

[1]Department of Pharmaceutics and Clinical Pharmacy, Faculty of Pharmacy, Sohag University, Sohag, 82524, Egypt; [2]Department of Pharmaceutics, Faculty of Pharmacy, Assiut University, Assiut, 71526, Egypt; [3]Department of Pharmaceutics, Faculty of Pharmacy, South Valley University, Qena, 83523, Egypt

Correspondence: Aml I Mekkawy, Department of Pharmaceutics and Clinical Pharmacy, Faculty of Pharmacy, Sohag University, Sohag, 82524, Egypt, Email aml.mekkawy@pharm.sohag.edu.eg



**Background:** Inflammation is the keystone in the disease's pathological process in response to any damaging stimuli. Therefore, any agent that inhibits the inflammatory response is under focus, either a drug or a bioactive compound. Selenium nanoparticles have drawn attention in various biomedical applications, including the anti-inflammatory activity.

**Purpose:** In the current study, we aimed to evaluate the capacity of different surface coating materials (soybean lecithin, PEG 6000, and β-cyclodextrin) to enhance the anti-inflammatory activity of the synthesized selenium nanoparticles (SeNPs). The capability of the coated SeNPs to adsorb indomethacin (IND) on their surfaces compared to the uncoated SeNPs was also evaluated.

**Methods:** SeNPs were synthesized, coated with different materials, and characterized in vitro using X-ray diffraction, UV-Vis spectrophotometer, FTIR, SEM, TEM, and particle size and zeta potential measurements. The in vivo anti-inflammatory activity of the uncoated/coated SeNPs loaded into hydrogel was evaluated using a carrageenan-induced paw edema rat model. The effect of SeNPs surface coatings was further evaluated for IND loading capacity.

**Results:** Our findings proved the superior anti-inflammatory activity of all coated SeNPs compared to the uncoated SeNPs, especially with β-cyclodextrin surface coating. Regarding the IND loading capacity of the prepared uncoated/coated SeNPs, the amount of drug loaded was 0.12, 1.12, 0.3, and 0.14 µg IND/µg SeNPs for the uncoated, lecithin-, PEG- and β-CD-coated SeNPs, respectively.

**Conclusion:** Surface functionalization of SeNPs can provide a synergistic therapeutic activity. Our results are promising for further investigation of the in vivo anti-inflammatory synergistic activity of the IND-loaded surface-coated SeNPs.

**Keywords:** selenium nanoparticles, soybean lecithin, polyethylene glycol, β-cyclodextrin, indomethacin, synergistic activity, carrageenan

## Introduction

The development of pathological conditions such as osteoarthritis, atherosclerosis, and ischemia are triggered by inflammation.[1] Therefore, agents that inhibit inflammation are medically beneficial in preventing disease progression. Even though many different drugs are used to treat inflammation, either steroidal (SAIDs) or nonsteroidal anti-inflammatory drugs (NSAIDs), they exhibit several adverse effects.[2] Obesity, osteoporosis, and sodium retention may result from using SAIDs, causing severe health problems, while gastrointestinal ulcers and hepatotoxicity are the most common side effects of the NSAIDs. Moreover, previous clinical studies have reported local adverse effects in 6.3% of participants after local application of NSAIDs, including irritation at the application site, redness, and itching.[3] In general, many researchers have developed new formulations to enhance the anti-inflammatory activity of drugs and decrease their side effects.[4]

Received: 14 February 2022
Accepted: 28 May 2022
Published: 13 June 2022

**Graphical Abstract**

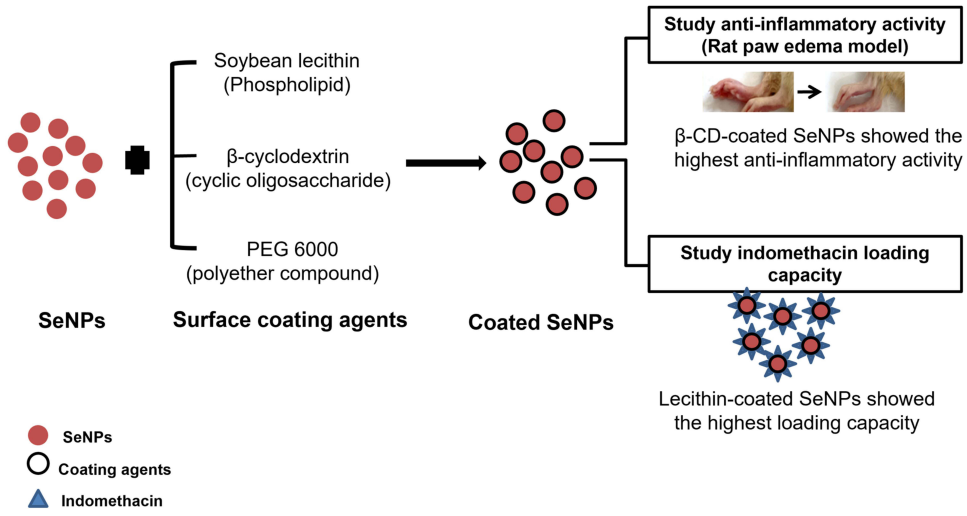


Metal nanoparticles, including selenium, have drawn attention in various biomedical applications.[5–7] Selenium exists in different oxidation states and chemical forms, including selenite, selenate, elemental selenium, and organic selenium compounds.[8,9] The narrow margin between beneficial and toxic doses of selenium controls its use;[10] the reported dose for extreme selenium toxicity is 2400 µg/day.[11] Selenium nanoparticles (SeNPs) are considered of low or no cytotoxicity compared to other Se forms, with interesting biological activity and bioavailability as elemental SeNPs possess high selenium density that allows local delivery of high doses into the site of action.[12–19] SeNPs show promising prospects because of their widespread biomedical applications, including anticancer,[20–22] anti-inflammatory,[10] antioxidant,[19,23,24] and antimicrobial activity,[23,25,26] treatment of arthritis,[27] cerebral strokes,[28] and psoriasis.[29] Applications of SeNPs are attributed to their antioxidant-mediated anti-inflammatory properties; they could downregulate the inflammatory mediators,[30] improve the oxidative stress-mediated inflammation, and enhance the antioxidant defense.[31–33]

The potential of SeNPs could be attributed to their concentration, nano-size range, and surface coating materials. Surface coating agents are attracting considerable interest to improve the efficacy and stability of metal nanoparticles as they impart their hydrophilic/hydrophobic nature to the surface of nanoparticles. A delicate balance between the two properties of the coating material could provide good water dispersibility, stability, and permeation.[34–36] Furthermore, the anti-inflammatory activity and safety profile of SeNPs could be augmented by surface decoration.[37,38] Lower toxicity was reported with polysaccharides-capped SeNPs compared to sodium selenium and selenium methionine.[39] Similarly, dextrin-coated SeNPs exhibited lower cytotoxicity (15%) compared to uncoated nanoparticles and sodium selenite (35% and 95%, respectively).[40] That noticeable decrease in the cytotoxicity of Se indicates changes in its properties after the formation of nanoparticles and their surface coating. Additionally, enhanced antimicrobial activity,[41] antioxidant,[42] and immunostimulant activity[43] were reported with surface functionalization of SeNPs using different materials including polyacrylic acid, polyvinylpyrrolidone, poly-L-lysine, chitosan, and β-Glucan. Moreover, the permeability of SeNPs through the blood-brain barrier was enhanced by modifying their surface using sialic acid and conjugation with B6 peptide to manage Alzheimer's disease.[44]

Therefore, precise selection of the surface coating material type is essential according to the planned purpose for metal nanoparticles coating. In the current study, we aimed to evaluate the impact of three different surface coating agents: soybean lecithin, polyethylene glycol (PEG 6000), and β-cyclodextrin (β-CD). Lecithin and PEG are regarded as suitable skin permeation enhancers.[45,46] In addition, lecithin (natural lipid mixture) is usually used as a stabilizing agent and a component of various delivery systems due to its safety and biocompatibility.[47–49] Besides, lecithin enhances the

anti-inflammatory activity of different drugs;[50] that could be attributed to 1,2-Dilinoleoyl-sn-glycero-3-phosphocholine (DLPC), which is the major and the most effective component of lecithin. The anti-inflammatory activity of DLPC was previously reported; it could diminish the proinflammatory cytokines, inhibit inducible nitric oxide synthase (iNOS) expression, decrease nitric oxide (NO) and tumor necrosis factor-alpha production.[51] CDs were previously used with anti-inflammatory drugs to enhance their stability, solubility, bioavailability, and activity;[52] this could highlight the vital role of β-CD in the anti-inflammatory processes.[52,53] PEG was previously conjugated with anti-inflammatory drugs to improve their activity. Researchers assumed that the enhanced activity resulting after PEG conjugation was due to the anti-inflammatory properties of PEG per se.[54] Based on the previous information, we sought first to prepare SeNPs coated with lecithin, PEG 6000, and β-CD. Then, we aimed to formulate a topically applied uncoated/coated SeNPs loaded hydrogel. We used this formulation to evaluate the potential of applying the lecithin, PEG 6000, and β-CD coated SeNPs as a promising anti-inflammatory therapy using the carrageenan-induced paw edema model. To the best of our knowledge, this is the first study that reports enhancing the anti-inflammatory activity of topically applied hydrogel loaded with SeNPs using lecithin, PEG 6000, and β-CD as surface coating agents. We also evaluated the potential of surface coating agents on the indomethacin (IND) loading capacity of SeNPs. Loading of IND to the surface of the coated SeNPs may provide a promising formulation with synergistic anti-inflammatory activity due to the combinatorial application of IND and the surface-coated SeNPs.

# Materials and Methods

## Materials

Sodium selenite, indomethacin, β-cyclodextrin (β-CD), Pluronic® F127 (PF-127), soybean lecithin, bovine serum albumin (BSA), carrageenan and glutathione (GSH) were purchased from Sigma (St Louis, MO, USA). Polyethylene glycol (PEG 6000) was purchased from Adwic, EL-Nasr Pharmaceutical Chemicals (Cairo, Egypt). All other chemicals and solvents used were of analytical grade.

## Methods

### Preparation of SeNPs

SeNPs were prepared according to Zhang, Gao, Zhang, Bao[14] with some modifications. First, a 25 mM sodium selenite solution in double distilled water (DDW) was added to 25 mM GSH solution containing 50 mg BSA. Then, SeNPs were formed directly after adjusting pH to 7.2 using 1.0 M sodium hydroxide. The dispersion was then dialyzed using a Spectra/Por® dialysis membrane (MWCO=12000-14,000; Spectrum Laboratories Inc., USA) against DDW for 96 h, at room temperature (25°C) with water being changed every day. Finally, SeNPs dispersions were lyophilized and stored for further characterizations.

### X-Ray Diffraction (XRD)

The X-ray diffraction pattern of the SeNPs powder was examined using an X-ray diffractometer (Model PW 1710, Philips, Amsterdam, the Netherlands). Measurements were swapped from 2θ=4° to 2θ=80° with a scanning speed of 0.06°/min.

### UV–Visible Spectrophotometry

The prepared SeNPs dispersion (250 µg/mL) in DDW was scanned from 200 to 500 nm wavelength using Thermo Scientific Evolution™ 300 UV–Vis Spectrophotometer (Thermo Fisher Scientific, Waltham, MA, USA).

### Evaluation of SeNP Morphology

The shape and surface morphology of SeNPs were determined using a scanning electron microscope (SEM, Hitachi, Japan). In brief, the lyophilized SeNPs were added onto a silicon wafer mounted on an aluminum SEM stub, and then coated with gold and palladium using an argon beam K550 sputter coater (Emitech Ltd, Kent, England). Images were captured by SEM operated at a 3 kV accelerating voltage.

### Transmission Electron Microscopy (TEM)

Briefly, a drop of the prepared SeNPs dispersion in DDW was placed on a carbon-coated copper grid and allowed to air dry. JEOL 100 CX II TEM (Tokyo, Japan) was used to image the sample at the Electron Microscopy Unit, Assiut University, Egypt. The size distribution of the nanoparticles was also evaluated.

### Surface Coating of SeNPs

Different surface coating agents were applied to SeNPs. The coating agents: 10 mM PEG 6000, 0.6% w/v soybean lecithin, and 10 mM β-CD were added separately to 250 µg/mL SeNPs dispersion in DDW to obtain the required final concentration of each coating agent. The dispersions were left stirring overnight at room temperature (25°C). Then, they were sonicated for 10 min using an ultrasonicator (Crest Ultrasonics Corp., Trenton, NJ, USA).

### Dynamic Light Scattering (DLS) and Zeta-Potential Measurements

The average hydrodynamic diameters, size distribution (polydispersity indices, PDIs), and zeta-potential values of the prepared uncoated/coated SeNPs dispersions in DDW were determined using a Malvern Zetasizer Nano series ZS instrument (Malvern Instruments, Malvern, UK).

### Fourier Transformed Infrared Spectroscopy (FTIR)

Infrared spectra of the dried uncoated/coated SeNPs, and pure powders of BSA, PEG 6000, lecithin, and β-CD were recorded using a Nicolet 6700 FT-IR spectrometer (Thermo Fisher Scientific, Waltham, MA).

### Formulation of SeNPs-Loaded Hydrogel

Four hydrogel formulations loaded with different uncoated/coated SeNPs (500 µg/mL) were prepared using 25% w/v PF-127 as a gelling agent. PF-127 hydrogels were prepared by the cold method described by Schmolka.[55] PF-127 powder was dissolved in cold dispersions of uncoated/coated SeNPs in DDW. Finally, the dispersions were refrigerated overnight, and clear transparent hydrogels were obtained at room temperature.

### In vivo Anti-Inflammatory Activity Study

The animal experiment was performed according to the ethical guidelines approved by the Institutional Animal Ethical Committee of the Faculty of Pharmacy, Assiut University (approval number: S22-21; approval date: 8 November 2021), which adheres to the Guide for the Care and Use of Laboratory Animals, 8th Edition, National Academies Press, Washington, DC, USA.

### Evaluation of Paw Edema Reduction Degree in Rats Over Time

Carrageenan-induced rat paw edema model is used to study the effect of the uncoated/coated SeNPs in reducing the inflammatory response. Eighteen adult rats aged 8–10 weeks and weighing ~200 g were used. Rats were randomly divided into six groups (each group containing three rats): Normal (healthy), negative control (carrageenan-injected with no treatment), SeNPs-loaded hydrogel, lecithin-, PEG-, and β-CD-coated SeNPs loaded hydrogel groups (2.55 mg/kg)[10,56] (Table 1). Paw edema was induced by injection of 0.1 mL of 1% w/v carrageenan suspension in normal saline into the rat paw

**Table 1** Experimental Treatment Groups Used in the Carrageenan-Induced Rat Paw Edema

| Group No. | Group Type | Treatment | No. of Rats |
|---|---|---|---|
| 1 | Healthy group (normal) | – | 3 |
| 2 | 1% w/v Carrageenan-injected (100 µL) | Untreated (negative control) | 3 |
| 3 | 1% w/v Carrageenan-injected (100 µL) | Uncoated-SeNPs (500 µg/mL) loaded hydrogel (F1) | 3 |
| 4 | 1% w/v Carrageenan-injected (100 µL) | Lecithin-coated SeNPs (500 µg/mL) loaded hydrogel (F2) | 3 |
| 5 | 1% w/v Carrageenan-injected (100 µL) | PEG-coated SeNPs (500 µg/mL) loaded hydrogel (F3) | 3 |
| 6 | 1% w/v Carrageenan-injected (100 µL) | β-CD-coated SeNPs (500 µg/mL) loaded hydrogel (F4) | 3 |

intraplantar tissue 1 h after the local administration of the studied formulations. The paw edema was assessed by measuring the thickness of the carrageenan injected paw (the right paw) using caliper[57] before and 1, 2, 3, 4, and 5 h after the intraplantar injection of carrageenan and expressed in millimeters (mm). Values are expressed as mean ± S.D.

### Hematological Examination

Blood samples were collected from the animals in heparinized vials and centrifuged at 4000 rpm for 15 min. Finally, the white blood cells (WBCs) were measured using the hematology analyzer.

### Histopathological Examination

Morphological alterations of tissues were assessed after the termination of the in vivo study using the light microscope. Rats were euthanized by cervical dislocation; the tissue samples from the right hind paws were harvested and processed for histological examination. Small pieces of the tissue were fixed in neutral buffered formalin (10% v/v, pH 7.2), dehydrated in graded series of ethanol, and cleared in methyl benzoate. Then, they were embedded in paraffin wax; thin paraffin sections (5 µm) were prepared and stained with Harris's hematoxylin and eosin. Tissue sections were evaluated for dermal edema, blood vessel congestion, and inflammatory cells infiltration.[6]

### Preparation and Characterization of IND-Loaded SeNPs

Dispersions of uncoated/coated SeNPs loaded with IND have been synthesized by a dropwise addition of a methanolic solution of IND (300 µg) to 250 µg/mL SeNPs (uncoated/coated) dispersions in DDW with continuous stirring overnight at room temperature (25°C). The IND-loaded uncoated SeNPs dispersion was scanned spectrophotometrically, and its shape and surface morphology were examined using SEM.

### Effect of Different Coating Materials on the Drug Loading Capacity

The drug loading capacity of uncoated/coated SeNPs was determined by the indirect method. The previously formed dispersion was centrifuged (Centurion Scientific Ltd., W. Sussex, UK) at 18,000 rpm, and the drug content was assessed in the supernatant. The IND concentration was measured spectrophotometrically at 320 nm and determined using a previously constructed calibration curve. The loading capacity was calculated using the following equation:[58]

$$\text{Loading capacity } (\mu g/\mu g) = \frac{(\text{Initial amount of drug} - \text{free drug that remained in the supernatant})}{\text{amount of the SeNPs carrier}}$$

### Statistical Analyses

GraphPad Prism software for Windows version 8.3.0 (GraphPad Software Inc.) was used for the statistical analyses. The one-way analysis of variance (ANOVA) followed by the Tukey post hoc test was performed to compare the average particle size, the drug loading between the differently coated SeNPs, and the in vivo anti-inflammatory activity between different groups. The right paw thickness data from the different animal groups were also subjected to one-way ANOVA using permutation test with the coin, rcompanion and multcompView packages in R software version 4.1.3 (R Core Team, 2022). Two-way ANOVA with permutation test was also performed to study the main effects of treatment (uncoated SeNPs- and lecithin-, PEG-, and β-CD-coated SeNPs loaded hydrogel) and time (1, 2, 3, 4, and 5 h) factors and their interactions on the percent inhibition of paw edema using R software and different solutions (Manly's approach, Edgington's approach, Still and White's permutation of residuals and ter Braak' method) versus the parametric F. These permutation analyses were carried out due to the small sample size which is considered a limitation in the in vivo anti-inflammatory study.

# Results

## Synthesis and Characterization of SeNPs

The production of SeNPs was recognized by visual detection of color transformation from transparency to red color (Figure 1A). The SeNPs dispersion was characterized by X-ray diffraction and UV-Vis spectrophotometry. The most distinguished reflections at 2Θ values 23.6, 45.5, 53.2, 71.9 in the XRD pattern correspond to the (100), (111), (201), and (113) relative emission intensity of the SeNPs were displayed, respectively (Figure 1B). The UV-Vis spectrum showed a peak absorbance at 254 nm (Figure 1C), representing the synthesis of spherical SeNPs, which matches previous studies.[59] A photographic image of the lyophilized SeNPs

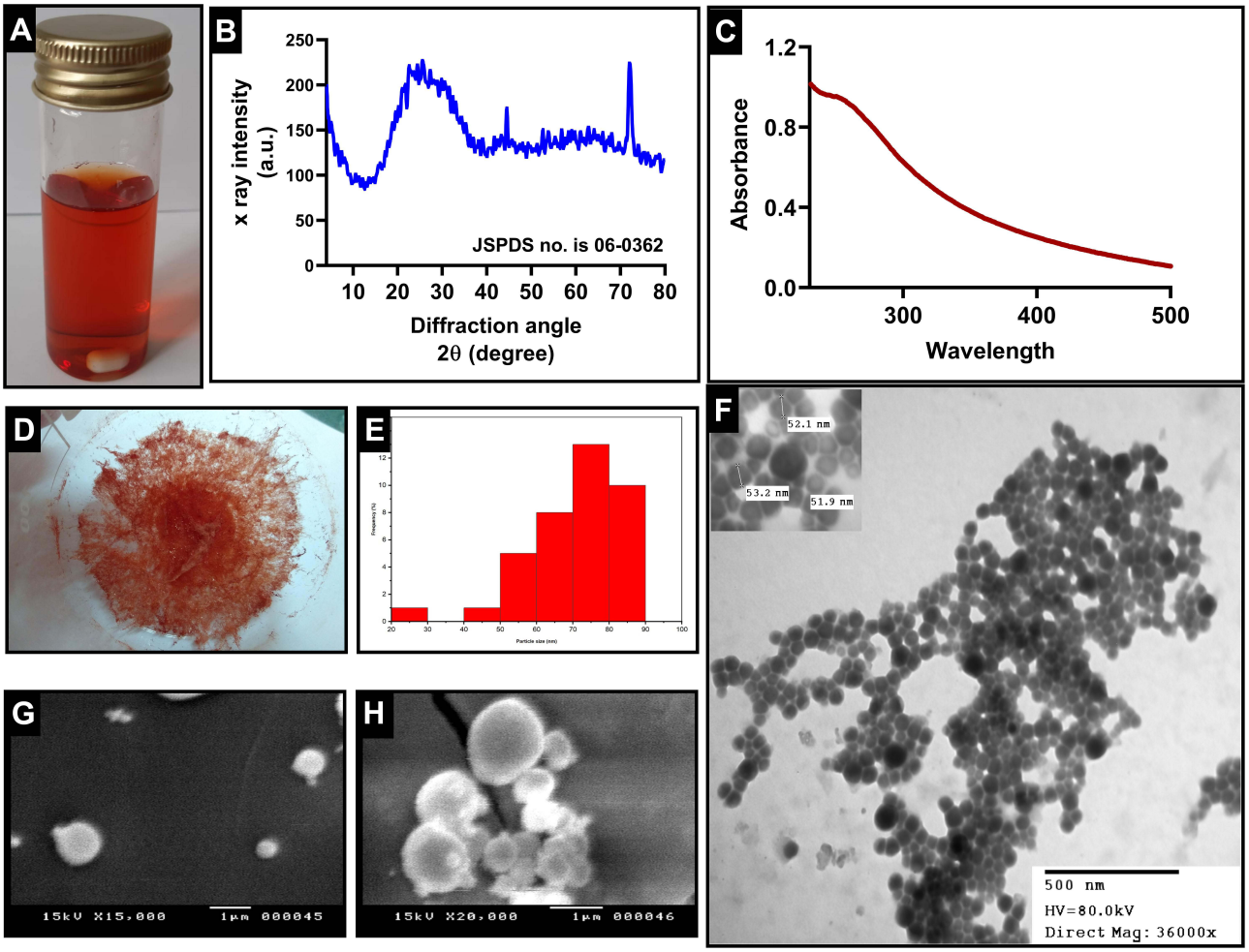


**Figure 1** Characterization of the synthesized SeNPs. (**A**) Color change from colorless solution to the red-colored dispersion of SeNPs. (**B**) X-ray diffraction pattern of the synthesized SeNPs. (**C**) UV-Visible spectrum of the synthesized SeNPs. (**D**) Photographic image of lyophilized SeNPs. (**E**) Histogram of SeNPs size distribution. (**F**) Representative TEM micrographs for the aqueous SeNPs dispersion (250 μg/mL). (**G** and **H**) Representative SEM micrographs for the dried SeNPs (250 μg/mL).
**Abbreviations**: SeNPs, selenium nanoparticles; SEM, scanning electron microscopy; TEM, transmission electron microscopy.

is shown in Figure 1D. The morphology and size of the SeNPs were determined using DLS, SEM, and TEM. Representative TEM micrographs of SeNPs with particle size distribution revealed diameters in the range of 40–90 nm (Figure 1E and F). The morphology of the synthesized SeNPs was examined using SEM and showed spherical-shaped particles (Figure 1G and H). Also, SeNPs dispersion exhibited a good monodispersity and size distribution with an average hydrodynamic diameter of 86.7 nm (obtained by dynamic light scattering; DLS) (Table 2).

**Table 2** Characterizations of the SeNPs Dispersions in Terms of Average Particle Size (Measured by Using DLS), PDI, and Zeta-Potential

| SeNPs Dispersion | DLS: Average Particle Size (nm) ± SD | DLS: Average PDI ± SD | Zeta-Potential (mV) ± SD |
|---|---|---|---|
| **Uncoated SeNPs** | 86.7 ± 5.0 | 0.2 ± 0.1 | −19.8 ± 1.9 |
| **Lecithin-coated SeNPs** | 125.7 ± 0.6 | 0.4 ± 0.0 | −43.7 ± 1.2 |
| **PEG-coated SeNPs** | 119.0 ± 2.0 | 0.3 ± 0.0 | −14.0 ± 1.3 |
| **β-CD-coated SeNPs** | 104.3 ± 6.7 | 0.4 ± 0.1 | −18.7 ± 2.2 |

## Characterization of Coated SeNPs Using Different Coating Materials

The surface coating of nanoparticles was confirmed by size and zeta potential changes and FTIR spectra. The dynamic light scattering and zeta potential measurements of uncoated/coated SeNPs are presented in Table 2. The average particle size of SeNPs (86.7 nm) increased significantly ($P<0.001$) after coating using lecithin, PEG 6000, and β-CD (125.7, 119.0, and 104.3 nm, respectively) with PDIs less than 0.5.

In addition, the surface charge of SeNPs has changed after coating, where lecithin-coated SeNPs exhibited a significant increase ($P<0.001$) in the zeta-potential value (from −19.8 to −43.7 mV). FTIR spectra of SeNPs, PEG-, Lecithin-, and β-CD-coated SeNPs are presented in Figure 2. As shown in the overlap of the FTIR spectra of lecithin and the lecithin-coated SeNPs, all the characteristic bands of lecithin are still available in the lecithin-coated SeNPs spectrum: 1740 (ester carbonyl), 1630 (C=C), 1261, and 1044 $cm^{-1}$ (P-O-R bonds).[60,61] Similarly, the most characteristic bands of β-CD are all shown in the spectrum of the β-CD-coated SeNPs: 2925 (C-H), 1151, and 1023 $cm^{-1}$ (C-O-C).[62] The characteristic absorption peaks of PEG are also still present in the PEG-coated SeNPs spectrum: 2890 (C-H), 1200, and 1094 $cm^{-1}$ (C-O-C).[63] Minor peak shifts were observed in the spectra of the coated SeNPs; a slight blueshift of the hydroxyl group band of lecithin and β-CD by +24 (from 3384 to 3408 $cm^{-1}$) and +21 (from 3360 to 3381 $cm^{-1}$) were shown, respectively. In contrast, the hydroxyl group band of PEG was red-shifted by −35 (from 3436 to 3401 $cm^{-1}$).

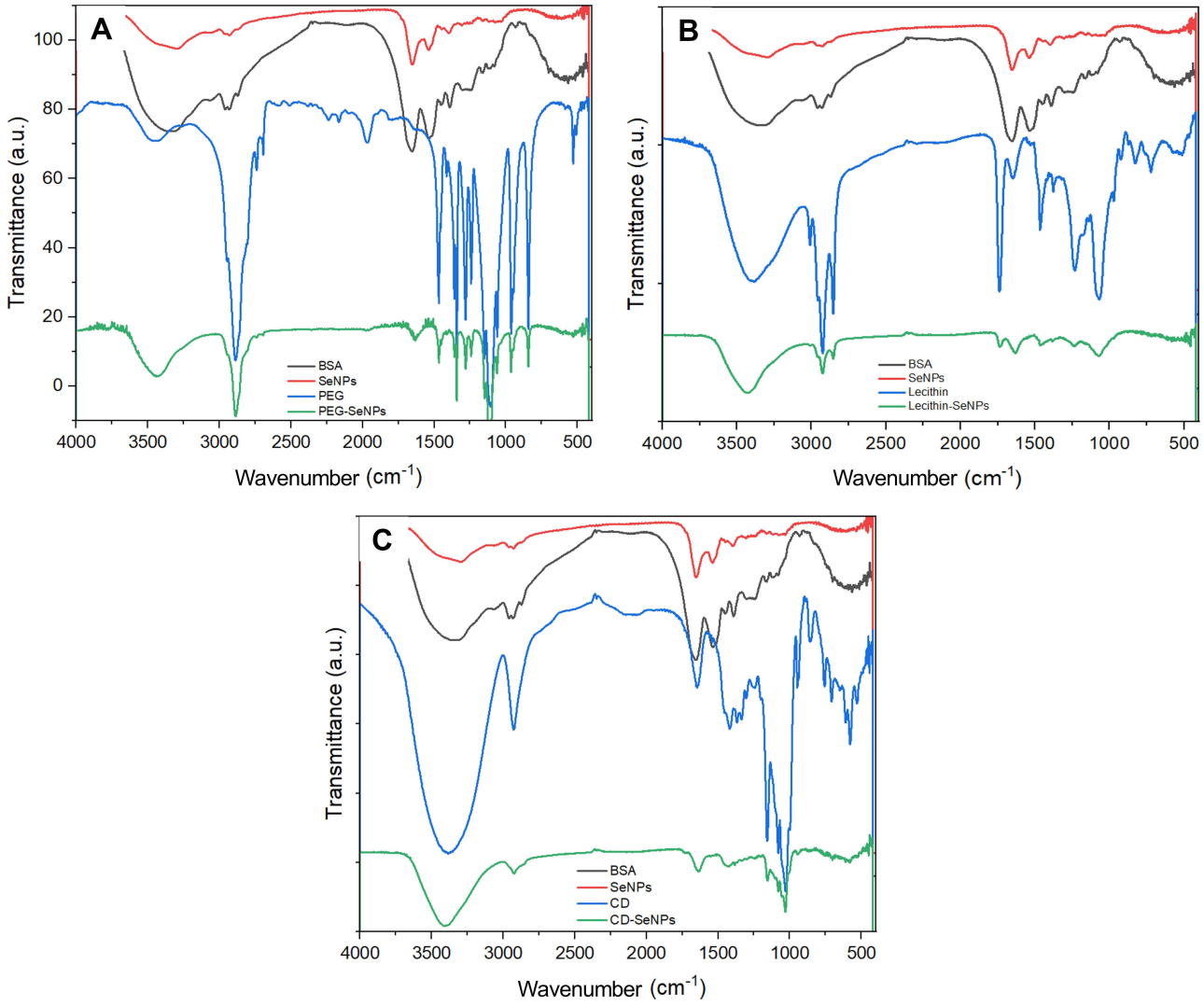


**Figure 2** FTIR spectra of BSA, SeNPs with (**A**) PEG-, (**B**) Lecithin-, and (**C**) β-CD-coated SeNPs.
**Abbreviations**: BSA, bovine serum albumin; SeNPs, selenium nanoparticles; PEG, polyethylene glycol; β-CD, β-cyclodextrin.

## Anti-Inflammatory Activity Study

### Carrageenan-Induced Paw Edema

Treatment of different animal groups using uncoated/coated SeNPs formulations reduced the paw edema development significantly ($P<0.001$) at all time points post carrageenan injection when compared to the negative control group (carrageenan-injected, with no treatment) (Figures 3 and 4). However, the permutation ANOVA revealed significant difference ($P<0.05$) between the paw thickness of the animal groups after 4 h only post carrageenan injection. Regarding the percent inhibition of paw edema, the main effects of the treatment and time factors were highly significant by the four solutions used ($P<0.00001$), and their interaction was also significant ($P=0.006$, 0.006, 0.0062, and 0.0058 for Manly's approach, Edgington's approach, Still and White's permutation of residuals and ter Braak' methods, respectively). As obviously noticed from photographic images in Figure 5, the β-CD-coated SeNPs treated group showed significant paw edema reduction when compared to lecithin- and PEG-coated SeNPs ($P<0.001$) 5 h post carrageenan injection. Interestingly, the β-CD-coated SeNPs treated group exhibited 41% and 54.2% paw edema reduction in the first and fourth hour, respectively, post carrageenan injection (Figure 4).

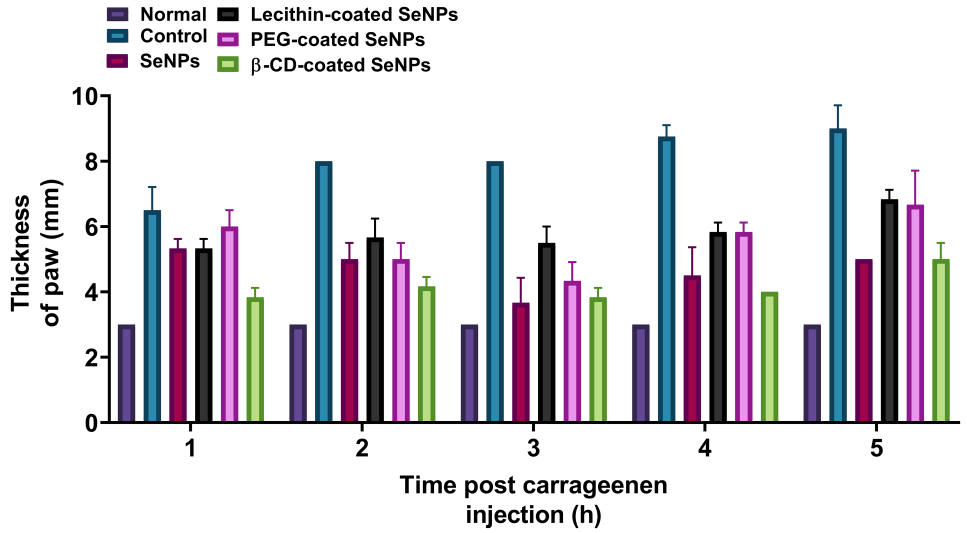


**Figure 3** The anti-inflammatory activity of different coated/uncoated SeNPs loaded in PF-127 hydrogel compared to the normal and negative control group (untreated), on carrageenan-induced right hind paw edema in rats. Paw size was measured every hour for 5 h. Data are expressed as mean ± SD (n=3). SeNPs, lecithin-, PEG- and β-CD-coated SeNPs treated groups showed a significant difference ($P < 0.001$) compared to the control group.

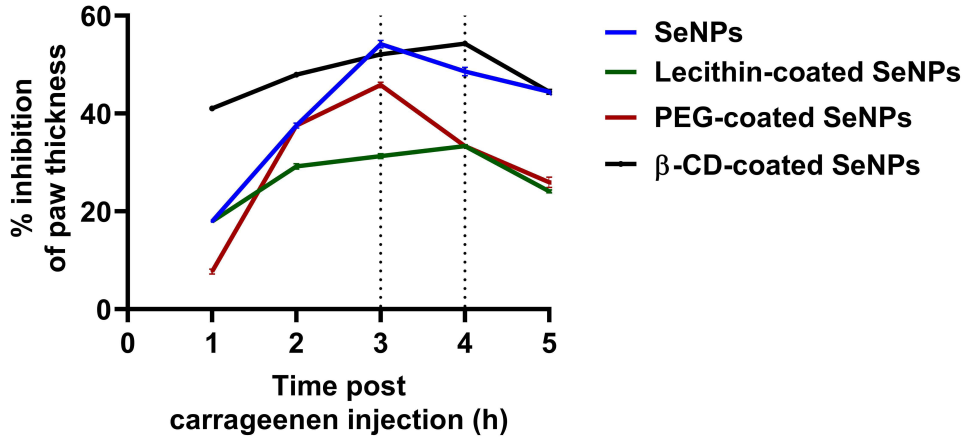


**Figure 4** Percent inhibition of paw thickness after topical application of different coated/uncoated SeNPs-loaded PF-127 hydrogel against negative control group (untreated) on carrageenan-induced right hind paw edema in rats. Paw size was measured every hour for 5 h. Data are expressed as mean ± SD (n=3).

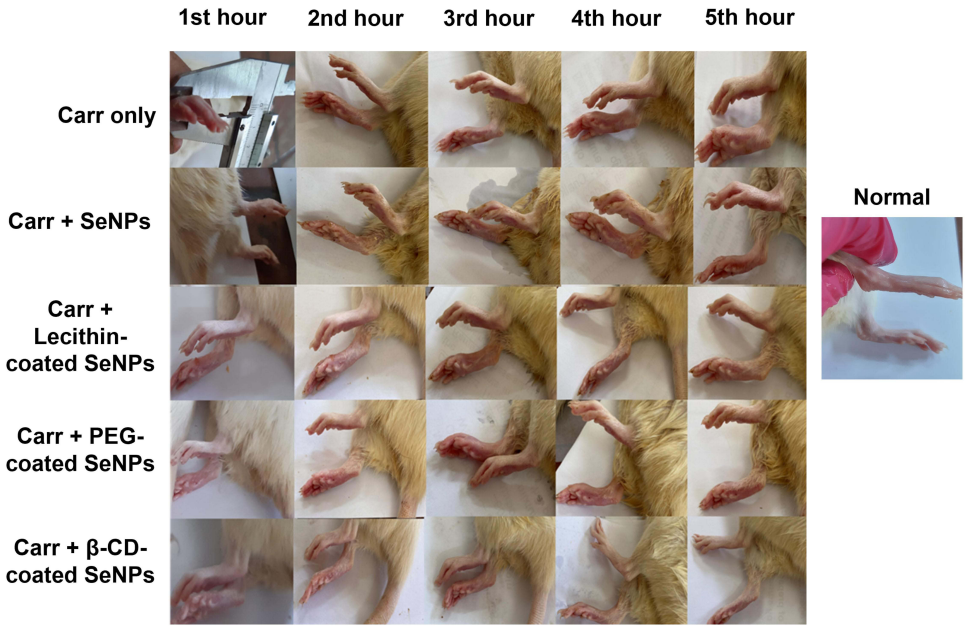


**Figure 5** Successive photographic images representing right rat paws at different time intervals to illustrate the anti-inflammatory activity of different coated/uncoated SeNPs-loaded PF-127 hydrogel against the normal and negative control group (untreated). Paw edema was induced by carrageenan injection into the rat paw intraplantar tissue 1 h after the topical administration of different formulations.

## Hematological Examination

The total number of WBCs in the blood was assessed 5 h post carrageenan injection. In the carrageenan injected group (negative control, untreated), WBCs were markedly increased (12-fold increase, 12,600 cells/mm$^3$) compared to the normal (healthy) group (1010 cells/mm$^3$) (Figure 6). Pretreatment of animal groups using the uncoated SeNPs, lecithin-, PEG-, and β-CD-coated SeNPs reduced WBCs count by approximately 31%, 50%, 44%, and 67%, respectively.

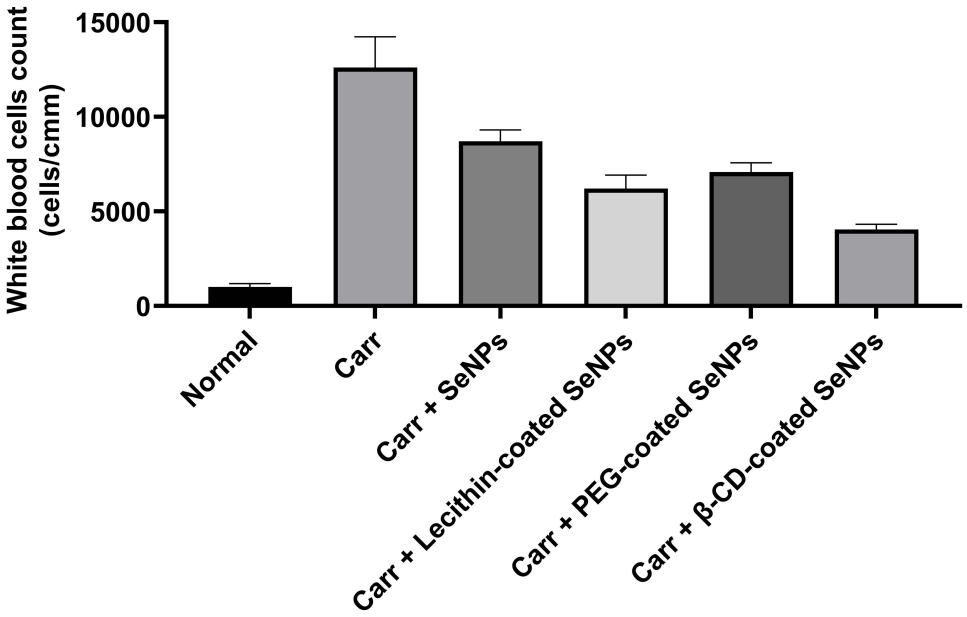


**Figure 6** Representative histogram showing white blood cells count (cells/cmm) in the blood 5 h post carrageenan intraplantar injection in the differently treated animal groups. Data are expressed as mean ± SD (n=3).
**Abbreviations**: Carr, carrageenan; SeNPs, selenium nanoparticles; PEG, polyethylene glycol; β-CD, β-cyclodextrin.

### Histopathological Examination

Paw sections of the normal (healthy) group showed no inflammatory cells and absence of any dilated blood vessels (Figure 7A$_{1,2}$). In contrast, sections from the carrageenan-injected group (negative control, untreated) showed congested blood vessels and nearby perivascular inflammatory cells (Figure 7B$_{1,2}$). After examining sections from the SeNPs-treated group (Figure 7C$_{1,2}$), mild dermal edema, slightly dilated blood vessels, and a few inflammatory cells were observed. Sections from the lecithin-coated SeNPs treated group (Figure 7D$_{1,2}$) showed mild inflammatory cells infiltrate. In contrast, sections from the PEG- and β-CD-coated SeNPs treated groups (Figure 7E$_{1,2}$ and F$_{1,2}$, respectively) showed normal non-congested (dilated) blood vessels and connective tissue dermis free of any inflammatory cells.

## IND-Loaded Uncoated SeNPs Characterization

IND-surface loading of SeNPs was confirmed by UV-Vis spectrophotometer (Figure 8A). The morphology of the IND-loaded SeNPs was examined using SEM. The presented images showed the difference in surface morphology between the SeNPs (Figure 1G and H) and the IND-loaded SeNPs (Figure 8B and C).

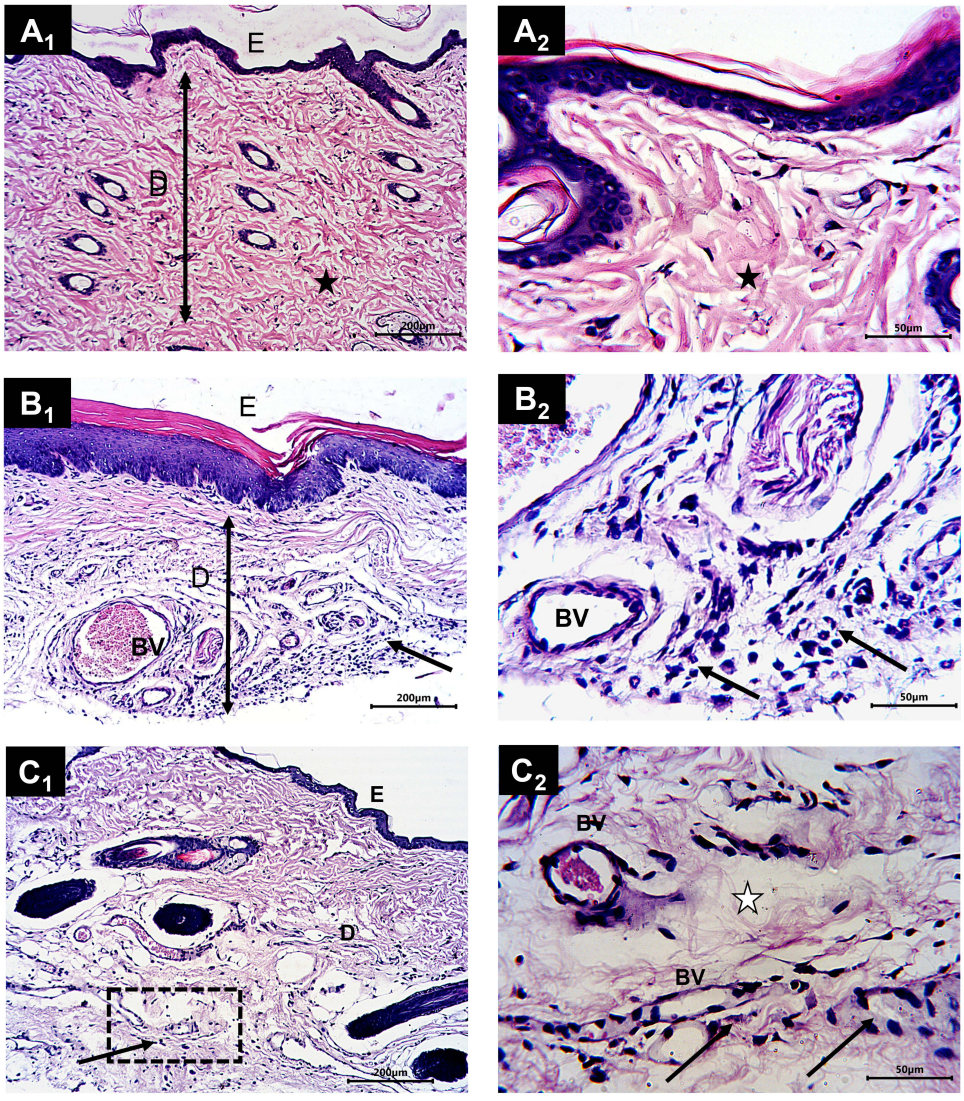


**Figure 7** Continue

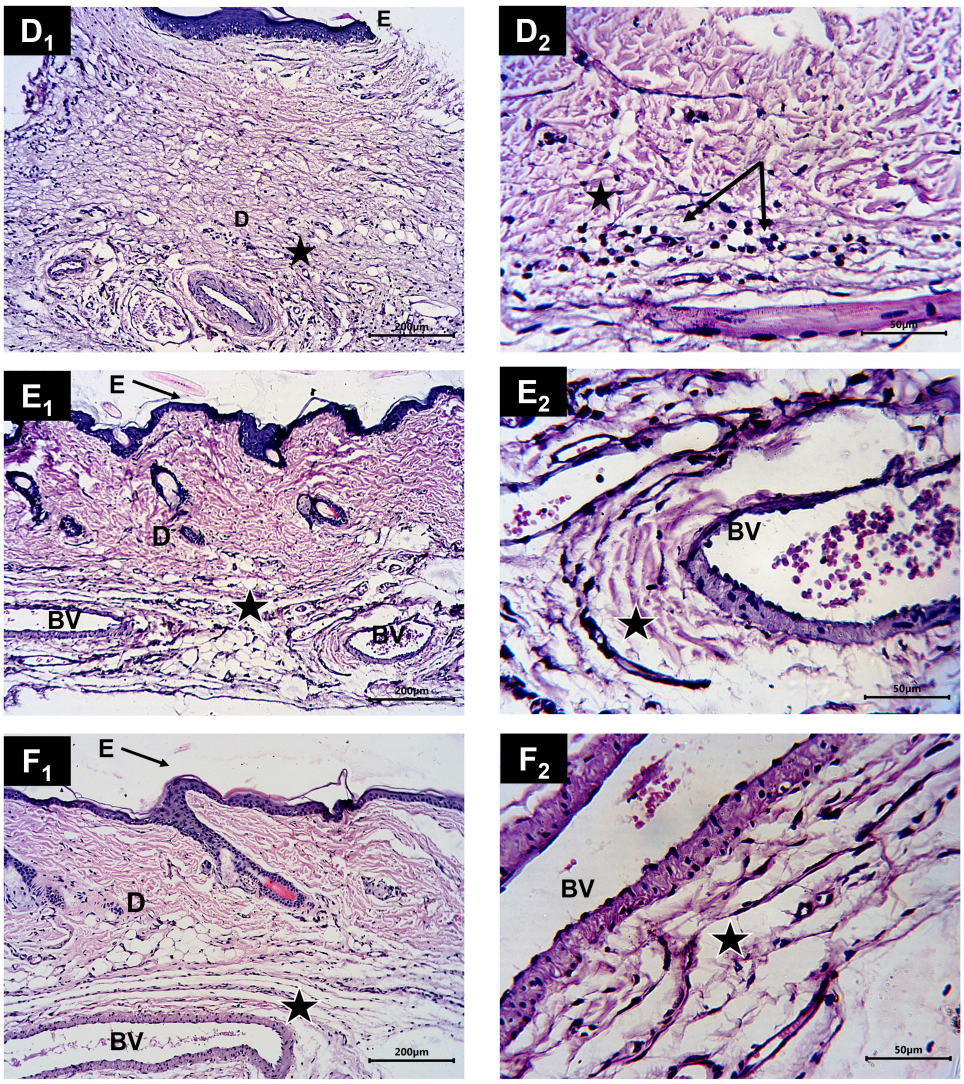


**Figure 7** Light microscopy images of representative rat paw tissue samples (stained with hematoxylin and eosin) and photographed at low power (x100, Bar = 200 μm) and high power (x400, Bar = 50μm), 5 h post carrageenan intraplantar injection of rat groups and administration of different treatments (**A1** and **2**) normal (healthy), (**B1** and **2**) untreated, (**C1** and **2**) SeNPs-loaded hydrogel (500 μg/mL), (**D1** and **2**) lecithin- coated SeNPs, (**E1** and **2**) PEG- and (**F1** and **2**) β-CD-coated SeNPs groups. E, D and BV represent epidermis, dermis, and blood vessels, respectively. Arrows refer to inflammatory cells, black stars refer to no inflammatory cells, and white star refers to mild dermal edema.
**Abbreviations**: SeNPs, selenium nanoparticles; PEG, polyethylene glycol; β-CD, β-cyclodextrin.

## Determination of IND Loading Capacity

The amount of IND loaded on the surface of the uncoated/coated SeNPs was determined by the indirect method. Results showed a loading capacity of 0.12 ± 0.1, 1.12 ± 0.06, 0.3 ± 0.07 and 0.14 ± 0.01 μg IND/μg SeNPs for the uncoated, lecithin-, PEG-, and β-CD-coated SeNPs, respectively. The lecithin-coated SeNPs showed a significant increase ($P$<0.001) in drug loading capacity compared to the uncoated, PEG-, and β-CD-coated SeNPs.

# Discussion

This study revealed the influence of surface coating materials: lecithin, PEG 6000, and β-cyclodextrin, on the anti-inflammatory activity and the IND loading capacity compared to the uncoated SeNPs. SeNPs dispersion was synthesized by reducing sodium selenite ($Na_2SeO_3$) with glutathione (GSH) using BSA as a colloidal stabilizing agent. The increased particle size confirmed the surface coating of SeNPs compared to the uncoated SeNPs. The small PDI (<0.5) of the uncoated/coated SeNPs revealed a uniform and homogenous particle size distribution.[6] The change in the surface charge of the coated SeNPs dispersions confirmed the formation of coated particles as well. The surface charge of the lecithin-coated SeNPs was

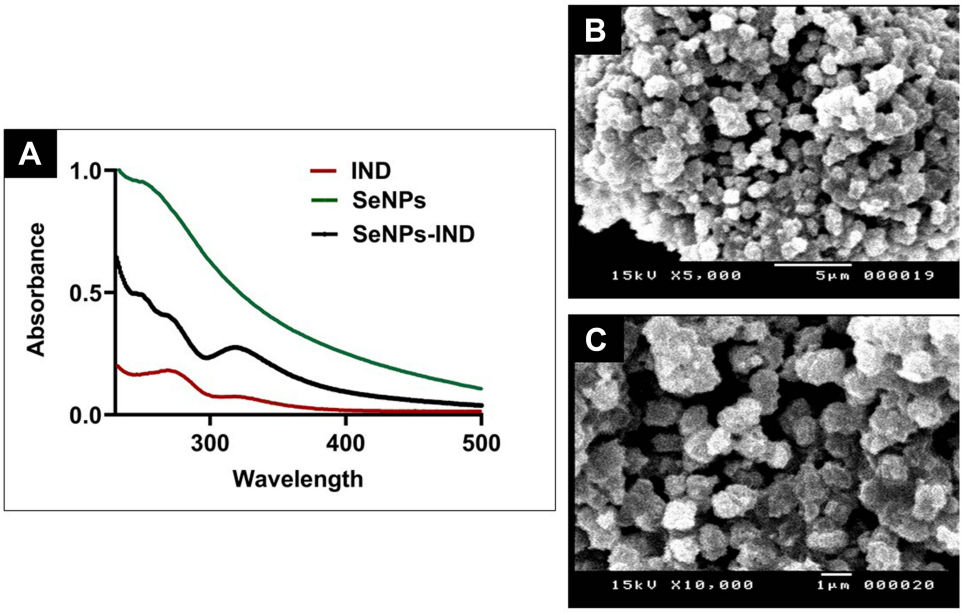


**Figure 8** (**A**) UV-Visible spectra of the synthesized SeNPs, IND, and IND-loaded SeNPs. (**B** and **C**) Representative SEM micrographs for the IND-loaded SeNPs.
**Abbreviations**: SeNPs, selenium nanoparticles; IND, indomethacin; SEM, scanning electron microscopy.

increased significantly due to the nature of lecithin, which is mainly amphipathic phosphatidylcholine molecules. In aqueous solution, lecithin makes a bilayer structure containing the aqueous SeNPs dispersion inside;[64] accordingly, the size, zeta potential, and stability of the nanoparticles were increased. Further confirmation was obtained from the FTIR spectra, where all the characteristic bands of the coating materials were available after SeNPs coating. The observed minor peak shifts indicated the physical interaction of coating materials and SeNPs through their hydroxyl group.[65,66] Additionally, the observed decrease in the intensity of other bands in the spectra of the coated SeNPs proved the surface coating of nanoparticles.[67]

Carrageenan-induced paw edema is the most used model in studying the acute inflammatory response in experimental animals; it induces the release of inflammatory mediators. Peripheral inflammation is developed after intraplantar carrageenan injection, leading to an increase in levels of interleukin 1, tumor necrosis factor α, prostaglandin E2, NO, iNOS, and cyclooxygenase-2 protein expression in the inflamed paw.[12,13] In the current study, we noticed that treatment using the formulations of uncoated/coated SeNPs (2.55 mg/kg) loaded in PF-127 hydrogel reduced the paw edema development at all time points compared to the untreated group. That could be attributed to the antioxidant activity of SeNPs which play a significant role in their anti-inflammatory activity.[16,23,68] Previous studies have reported the inhibitory activity of SeNPs on the accumulation of redox oxygen species and protection of glutathione peroxidase activity.[42,68] Therefore, the observed inhibition of paw edema development could be attributed to the inhibition of neutrophil infiltration that plays a vital role in the carrageenan-induced inflammation in the rat paw.[69] Noticeably, the β-CD-coated SeNPs treated group showed the highest reduction of paw edema from the first hour. CD inhibits the inflammatory mediators and reduces edema;[70] therefore, it could improve the activity of anti-inflammatory drugs.

Using light microscopy, we further examined paw tissue samples from the untreated/treated animal groups. The acute inflammation induced by intraplantar carrageenan injection includes two phases:[69] an early phase during the first hour of exposure and a delayed phase after the first hour of exposure which is recognized by infiltration of polymorphonuclear leucocyte.[71] We observed a reduction in the inflammatory cells in tissues from the SeNPs and the lecithin-coated SeNPs treated groups. In contrast, tissues from the β-CD- and PEG-coated SeNPs showed no inflammatory cells compared to those from the untreated group. Levels of WBCs count revealed the differences in response between untreated/treated animal groups 5 h post carrageenan injection.[72] The observed reduction in the inflammatory cells, together with the decrease in the WBCs count from hematological analysis, proved our hypothesis that the different coating materials augmented the anti-inflammatory activity of SeNPs with some variations.

The effect of the surface coating of SeNPs was further evaluated for IND loading capacity; this approach will provide a promising synergistic anti-inflammatory activity. Lecithin-coated SeNPs exhibited the highest IND loading capacity due to the electrostatic interaction between the negatively charged head group of phosphatidylcholines in lecithin and the positively charged IND.[73] Further investigations and future work will include the optimization of the current IND-loaded coated SeNPs, to increase the IND loading on the surface of the coated nanoparticles. Furthermore, we plan to study the in vivo synergistic anti-inflammatory activity between the anti-inflammatory drug, the SeNPs, and the surface coating materials in a drug-loaded surface-coated SeNPs formulation. Finally, we also plan to evaluate the safety profile of this combinatorial therapeutic approach.

## Conclusion

SeNPs have many biomedical applications, including anti-inflammatory and antioxidant activities. Moreover, coated SeNPs exhibit low toxicity, high activity, and bioavailability. The current work revealed the inhibitory effect of Lecithin-, PEG- and β-CD coated SeNPs on the inflammatory response after acute inflammation using the carrageenan-induced paw edema model in rats. β-CD-coated SeNPs showed the highest anti-inflammatory activity, characterized by reduced edema development associated with a decrease in the WBCs count in the blood. Lecithin-coated SeNPs displayed superior IND loading capacity. In general, our findings highlight the importance of surface coating agents of nanoparticles in improving their activity. This strategy may provide a promising synergistic therapeutic activity between the nanoparticles, the surface coating materials, and the surface-loaded drug.

## Acknowledgment

The authors gratefully acknowledge Prof. Dr. Soad Shaker Ali (Faculty of Medicine, Assiut University, Egypt) for her valuable cooperation in histological studies.

## Disclosure

The authors declare that they have no known competing financial interests or personal relationships that could have appeared to influence the work reported in this paper.

## References

1. Libby P, Ridker PM, Maseri A. Inflammation and atherosclerosis. *Circulation*. 2002;105(9):1135–1143. doi:10.1161/hc0902.104353
2. McCarberg B, Gibofsky A. Need to develop new nonsteroidal anti-inflammatory drug formulations. *Clin Ther*. 2012;34(9):1954–1963. doi:10.1016/j.clinthera.2012.08.005
3. Massey T, Derry S, Moore RA, McQuay HJ, Topical NSAIDs for acute pain in adults. *Cochrane Database Syst Rev*. 2010;6:Cd007402. doi:10.1002/14651858.CD007402.pub2
4. Janakiraman K, Krishnaswami V, Rajendran V, Natesan S, Kandasamy R. Novel nano therapeutic materials for the effective treatment of rheumatoid arthritis-recent insights. *Mater Today Commun*. 2018;17:200–213. doi:10.1016/j.mtcomm.2018.09.011
5. Jabir MS, Hussien AA, Sulaiman GM, et al. Green synthesis of silver nanoparticles from Eriobotrya japonica extract: a promising approach against cancer cells proliferation, inflammation, allergic disorders and phagocytosis induction. *Artif Cells, Nanomed Biotechnol*. 2021;49(1):48–60. doi:10.1080/21691401.2020.1867152
6. Mekkawy AI, El-Mokhtar MA, Nafady NA, et al. In vitro and in vivo evaluation of biologically synthesized silver nanoparticles for topical applications: effect of surface coating and loading into hydrogels. *Int J Nanomedicine*. 2017;12:759–777. doi:10.2147/IJN.S124294
7. Alizadeh S, Seyedalipour B, Shafieyan S, Kheime A, Mohammadi P, Aghdami N. Copper nanoparticles promote rapid wound healing in acute full thickness defect via acceleration of skin cell migration, proliferation, and neovascularization. *Biochem Biophys Res Commun*. 2019;517(4):684–690. doi:10.1016/j.bbrc.2019.07.110
8. Barceloux DG, Barceloux D. Selenium. *Journal of Toxicology: Clinical Toxicology*. 1999;37(2):145–172. doi:10.1081/CLT-100102417
9. Malyugina S, Skalickova S, Skladanka J, Slama P, Horky P. Biogenic selenium nanoparticles in animal nutrition: a review. *Agriculture*. 2021;11(12):1244. doi:10.3390/agriculture11121244
10. El-Ghazaly MA, Fadel N, Rashed E, El-Batal A, Kenawy SA. Anti-inflammatory effect of selenium nanoparticles on the inflammation induced in irradiated rats. *Can J Physiol Pharmacol*. 2017;95(2):101–110. doi:10.1139/cjpp-2016-0183
11. Navarro-Alarcon M, Cabrera-Vique C. Selenium in food and the human body: a review. *Sci Total Environ*. 2008;400(1–3):115–141. doi:10.1016/j.scitotenv.2008.06.024
12. Nagy G, Pinczes G, Pinter G, Pocsi I, Prokisch J, Banfalvi G. In situ electron microscopy of lactomicroselenium particles in probiotic bacteria. *Int J Mol Sci*. 2016;17(7):1047. doi:10.3390/ijms17071047
13. Deng G, Zhu T, Zhou L, et al. Bovine serum albumin-loaded nano-selenium/ICG nanoparticles for highly effective chemo-photothermal combination therapy. *RSC Adv*. 2017;7(49):30717–30724. doi:10.1039/C7RA02384G
14. Zhang JS, Gao XY, Zhang LD, Bao YP. Biological effects of a nano red elemental selenium. *Biofactors*. 2001;15(1):27–38. doi:10.1002/biof.5520150103

15. Ferro C, Florindo HF, Santos HA. Selenium nanoparticles for biomedical applications: from development and characterization to therapeutics. *Adv Healthcare Mater*. 2021;10(16):e2100598. doi:10.1002/adhm.202100598
16. Abdou RH, Sayed N. Antioxidant and anti-inflammatory effects of nano-selenium against cypermethrin-induced liver toxicity. *CellBio*. 2019;8:53–65. doi:10.4236/cellbio.2019.84004
17. Khalaf A, Ahmed W, Moselhy W, Abdel-Halim B, Ibrahim M. Protective effects of selenium and nano-selenium on bisphenol-induced reproductive toxicity in male rats. *Hum Exp Toxicol*. 2019;38(4):398–408. doi:10.1177/0960327118816134
18. Peng D, Zhang J, Liu Q, Taylor EW. Size effect of elemental selenium nanoparticles (Nano-Se) at supranutritional levels on selenium accumulation and glutathione S-transferase activity. *J Inorg Biochem*. 2007;101(10):1457–1463. doi:10.1016/j.jinorgbio.2007.06.021
19. Ndwandwe BK, Malinga SP, Kayitesi E, Dlamini BC. Advances in green synthesis of selenium nanoparticles and their application in food packaging. *Int J Food Sci Technol*. 2021;56(6):2640–2650. doi:10.1111/ijfs.14916
20. Huang Y, He L, Liu W, et al. Selective cellular uptake and induction of apoptosis of cancer-targeted selenium nanoparticles. *Biomaterials*. 2013;34 (29):7106–7116. doi:10.1016/j.biomaterials.2013.04.067
21. Guleria A, Baby CM, Tomy A, et al. Size tuning, phase stabilization, and anticancer efficacy of amorphous selenium nanoparticles: effect of ion-pair interaction, −OH functionalization, and reuse of RTILs as host matrix. *J Phys Chem C*. 2021;125(25):13933–13945. doi:10.1021/acs.jpcc.1c02894
22. Guleria A, Chakraborty S, Neogy S, Maurya DK, Adhikari S. Controlling the phase and morphology of amorphous Se nanoparticles: their prolonged stabilization and anticancer efficacy. *Chem Commun*. 2018;54(63):8753–8756. doi:10.1039/C8CC05375H
23. Boroumand S, Safari M, Shaabani E, Shirzad M, Faridi-Majidi R. Selenium nanoparticles: synthesis, characterization and study of their cytotoxicity, antioxidant and antibacterial activity. *Mater Res Express*. 2019;6(8):0850d0858. doi:10.1088/2053-1591/ab2558
24. Guleria A, Maurya DK, Neogy S, Raorane BS, Debnath AK, Adhikari S. A 10 minute approach for the phase specific synthesis of Se nanoparticles with tunable morphology: their anticancer efficacy and the role of an ionic liquid. *New J Chem*. 2020;44(11):4578–4589. doi:10.1039/C9NJ06088J
25. Filipović N, Ušjak D, Milenković MT, et al. Comparative study of the antimicrobial activity of selenium nanoparticles with different surface chemistry and structure. *Front Bioeng Biotechnol*. 2020;8:624621. doi:10.3389/fbioe.2020.624621
26. Gunti L, Dass RS, Kalagatur NK. Phytofabrication of selenium nanoparticles from emblica officinalis fruit extract and exploring its biopotential applications: antioxidant, antimicrobial, and biocompatibility. *Front Microbiol*. 2019;10. doi:10.3389/fmicb.2019.00931
27. Yazdi MH, Varastehmoradi B, Faghfuri E, Mavandadnejad F, Mahdavi M, Shahverdi AR. Adjuvant effect of biogenic selenium nanoparticles improves the immune responses and survival of mice receiving 4T1 cell antigens as vaccine in breast cancer murine model. *J Nanosci Nanotechnol*. 2015;15(12):10165–10172. doi:10.1166/jnn.2015.11692
28. Amani H, Habibey R, Shokri F, et al. Selenium nanoparticles for targeted stroke therapy through modulation of inflammatory and metabolic signaling. *Sci Rep*. 2019;9(1):6044. doi:10.1038/s41598-019-42633-9
29. Gangadevi V, Thatikonda S, Pooladanda V, Devabattula G, Godugu C. Selenium nanoparticles produce a beneficial effect in psoriasis by reducing epidermal hyperproliferation and inflammation. *J Nanobiotechnology*. 2021;19(1):101. doi:10.1186/s12951-021-00842-3
30. Mohamed AA, Zaghloul RA, Abdelghany AM, El Gayar AM. Selenium nanoparticles and quercetin suppress thioacetamide-induced hepatocellular carcinoma in rats: attenuation of inflammation involvement. *J Biochem Mol Toxicol*. 2022;36:e22989. doi:10.1002/jbt.22989
31. Rehman A, John P, Bhatti A. Biogenic selenium nanoparticles: potential solution to oxidative stress mediated inflammation in rheumatoid arthritis and associated complications. *Nanomaterials*. 2021;11(8):2005. doi:10.3390/nano11082005
32. Vieira AT, Silveira KD, Arruda MC, et al. Treatment with Selemax®, a selenium-enriched yeast, ameliorates experimental arthritis in rats and mice. *Br J Nutr*. 2012;108(10):1829–1838. doi:10.1017/S0007114512000013
33. Hassanin KM, Abd El-Kawi SH, Hashem KS. The prospective protective effect of selenium nanoparticles against chromium-induced oxidative and cellular damage in rat thyroid. *Int J Nanomedicine*. 2013;8:1713–1720. doi:10.2147/IJN.S42736
34. Fratoddi I. Hydrophobic and hydrophilic Au and Ag nanoparticles. breakthroughs and perspectives. *Nanomaterials*. 2017;8(1):11. doi:10.3390/nano8010011
35. Reboredo C, González-Navarro CJ, Martínez-Oharriz C, Martínez-López AL, Irache JM. Preparation and evaluation of PEG-coated zein nanoparticles for oral drug delivery purposes. *Int J Pharm*. 2021;597:120287. doi:10.1016/j.ijpharm.2021.120287
36. Cao D, Shu X, Zhu D, Liang S, Hasan M, Gong S. Lipid-coated ZnO nanoparticles synthesis, characterization and cytotoxicity studies in cancer cell. *Nano Converg*. 2020;7(1):14. doi:10.1186/s40580-020-00224-9
37. Ye R, Huang J, Wang Z, Chen Y, Dong Y. Trace element selenium effectively alleviates intestinal diseases. *Int J Mol Sci*. 2021;22(21):11708. doi:10.3390/ijms222111708
38. Wang J, Zhang Y, Yuan Y, Yue T. Immunomodulatory of selenium nano-particles decorated by sulfated Ganoderma lucidum polysaccharides. *Food Chem Toxicol*. 2014;68:183–189. doi:10.1016/j.fct.2014.03.003
39. Xu C, Qiao L, Ma L, et al. Biosynthesis of polysaccharides-capped selenium nanoparticles using Lactococcus*lactis* NZ9000 and their antioxidant and anti-inflammatory activities. *Front Microbiol*. 2019;10:1632. doi:10.3389/fmicb.2019.01632
40. Malhotra S, Welling MN, Mantri SB, Desai K. In vitro and in vivo antioxidant, cytotoxic, and anti-chronic inflammatory arthritic effect of selenium nanoparticles. *J Biomed Mater Res B Appl Biomater*. 2016;104(5):993–1003. doi:10.1002/jbm.b.33448
41. Galić E, Ilić K, Hartl S, et al. Impact of surface functionalization on the toxicity and antimicrobial effects of selenium nanoparticles considering different routes of entry. *Food Chem Toxicol*. 2020;144:111621. doi:10.1016/j.fct.2020.111621
42. Zhai X, Zhang C, Zhao G, Stoll S, Ren F, Leng X. Antioxidant capacities of the selenium nanoparticles stabilized by chitosan. *J Nanobiotechnology*. 2017;15(1):4. doi:10.1186/s12951-016-0243-4
43. Dung NT, Trong TD, Vu NT, Binh NT, Minh TTL, Luan LQ. Radiation synthesis of selenium nanoparticles capped with β-Glucan and its immunostimulant activity in cytoxan-induced immunosuppressed mice. *Nanomaterials*. 2021;11(9). doi:10.3390/nano11092439
44. Yin T, Yang L, Liu Y, Zhou X, Sun J, Liu J. Sialic acid (SA)-modified selenium nanoparticles coated with a high blood-brain barrier permeability peptide-B6 peptide for potential use in Alzheimer's disease. *Acta biomaterialia*. 2015;25:172–183. doi:10.1016/j.actbio.2015.06.035
45. Shah S, Safdar A, Riaz R, et al. Effect of permeation enhancers on the release behavior and permeation kinetics of novel tramadol lotions. *Trop J Pharmaceut Res*. 2013;12:27–32.
46. Puglia C, Rizza L, Offerta A, Gasparri F, Giannini V, Bonina F. Formulation strategies to modulate the topical delivery of anti-inflammatory compounds. *J Cosmet Sci*. 2013;64(5):341–353.
47. Hafner A, Lovrić J, Pepić I, Filipović-Grčić J. Lecithin/chitosan nanoparticles for transdermal delivery of melatonin. *J Microencapsul*. 2011;28 (8):807–815. doi:10.3109/02652048.2011.622053

48. Barani H, Montazer M, Toliyat T, Samadi N. Synthesis of Ag-liposome nano composites. *J Liposome Res*. 2010;20(4):323–329. doi:10.3109/08982100903544177
49. Barani H, Montazer M, Braun HG, Dutschk V. Stability of colloidal silver nanoparticles trapped in lipid bilayer: effect of lecithin concentration and applied temperature. *IET Nanobiotechnol*. 2014;8(4):282–289. doi:10.1049/iet-nbt.2013.0048
50. Esmaeili S, Omid-Malayeri S, Hajimehdipoor H, et al. The role of lecithin on topical anti-inflammatory activity of turmeric (Curcuma longa L.) ointment. *J Med Plants*. 2020;19(76):89–98. doi:10.29252/jmp.19.76.89
51. Son Y, Lee JH, Kim NH, et al. Dilinoleoylphosphatidylcholine induces the expression of the anti-inflammatory heme oxygenase-1 in RAW264.7 macrophages. *Biofactors*. 2010;36(3):210–215. doi:10.1002/biof.87
52. Jang S, Lee S, Park H. β-Cyclodextrin inhibits monocytic adhesion to endothelial cells through nitric oxide-mediated depletion of cell adhesion molecules. *Molecules*. 2020;25(16):3575. doi:10.3390/molecules25163575
53. Lucia Appleton S, Navarro-Orcajada S, Martínez-Navarro FJ, et al. Cyclodextrins as anti-inflammatory agents: basis, drugs and perspectives. *Biomolecules*. 2021;11(9):1384. doi:10.3390/biom11091384
54. Ackland G, Gutierrez Del Arroyo A, Yao S, et al. Low-molecular-weight polyethylene glycol improves survival in experimental sepsis. *Crit Care Med*. 2009;38:629–636. doi:10.1097/CCM.0b013e3181c8fcd0
55. Schmolka IR. Artificial skin. I. Preparation and properties of pluronic F-127 gels for treatment of burns. *J Biomed Mater Res*. 1972;6(6):571–582. doi:10.1002/jbm.820060609
56. Biswas S, Talukder G, Sharma A. Selenium salts and chromosome damage. *Mutat Res*. 1997;390(3):201–205. doi:10.1016/S1383-5718(97)00004-1
57. Morris CJ. Carrageenan-induced paw edema in the rat and mouse. *Methods Mol Biol*. 2003;225:115–121. doi:10.1385/1-59259-374-7:115
58. Gurunathan S, Raman J, Abd Malek SN, John PA, Vikineswary S. Green synthesis of silver nanoparticles using Ganoderma neo-japonicum Imazeki: a potential cytotoxic agent against breast cancer cells. *Int J Nanomedicine*. 2013;8:4399–4413. doi:10.2147/IJN.S51881
59. Chung S, Zhou R, Webster TJ. Green synthesized BSA-coated selenium nanoparticles inhibit bacterial growth while promoting mammalian cell growth. *Int J Nanomedicine*. 2020;15:115–124. doi:10.2147/IJN.S193886
60. Silva R, R. S. Lara L, López J. Preparation of magnetoliposomes with a green, low-cost, fast and scalable methodology and activity study against S aureus and C freundii bacterial strains. *J Braz Chem Soc*. 2018;29(12):2636–2645. doi:10.21577/0103-5053.20180144
61. Nurul Hidayah SS. The effect of papain enzyme dosage on the modification of egg-yolk lecithin emulsifier product through enzymatic hydrolysis reaction. *Int J Technol*. 2018;9(2):291–319.
62. Da Silva Júnior WF, Bezerra de Menezes DL, de Oliveira LC, et al. Inclusion Complexes of β and HPβ-Cyclodextrin with α, β amyrin and in vitro anti-inflammatory activity. *Biomolecules*. 2019;9(6):241. doi:10.3390/biom9060241
63. Biswal S, Sahoo J, Murthy PN, Giradkar RP, Avari JG. Enhancement of dissolution rate of gliclazide using solid dispersions with polyethylene glycol 6000. *AAPS PharmSciTech*. 2008;9(2):563–570. doi:10.1208/s12249-008-9079-z
64. Hosseini F, Sadjadi M. Synthesis and characterization of soy lecithin coated magnetic iron oxide nanoparticles for magnetic resonance imaging applications. *Orient J Chem*. 2016;32:2901–2908. doi:10.13005/ojc/320608
65. Huang T, Kumari S, Herold H, et al. Enhanced antibacterial activity of se nanoparticles upon coating with recombinant spider silk protein eADF4 (κ16). *Int J Nanomedicine*. 2020;15:4275–4288. doi:10.2147/IJN.S255833
66. Wang Z, Ji L, Ren Y, Liu M, Ai X, Yang C. Preparation and anti-tumor study of dextran 70,000-selenium nanoparticles and poloxamer 188-selenium nanoparticles. *AAPS PharmSciTech*. 2021;23(1):29. doi:10.1208/s12249-021-02141-4
67. Valizadeh H, Nokhodchi A, Qarakhani N, et al. Physicochemical characterization of solid dispersions of indomethacin with PEG 6000, Myrj 52, lactose, sorbitol, dextrin, and Eudragit E100. *Drug Dev Ind Pharm*. 2004;30(3):303–317. doi:10.1081/DDC-120030426
68. Amani H, Habibey R, Hajmiresmail SJ, Latifi S, Pazoki-Toroudi H, Akhavan O. Antioxidant nanomaterials in advanced diagnoses and treatments of ischemia reperfusion injuries. *J Mater Chem B*. 2017;5(48):9452–9476. doi:10.1039/C7TB01689A
69. Gilligan JP, Lovato SJ, Erion MD, Jeng AY. Modulation of carrageenan-induced hind paw edema by substance P. *Inflammation*. 1994;18(3):285–292. doi:10.1007/BF01534269
70. Santos PL, Brito RG, Quintans JSS, et al. Cyclodextrins as complexation agents to improve the anti-inflammatory drugs profile: a systematic review and meta-analysis. *Curr Pharm Des*. 2017;23(14):2096–2107. doi:10.2174/1381612823666170126121926
71. Shin S, Jeon JH, Park D, et al. Anti-inflammatory effects of an ethanol extract of Angelica gigas in a Carrageenan-air pouch inflammation model. *Exp Animals*. 2009;58(4):431–436. doi:10.1538/expanim.58.431
72. Zouari Bouassida K, Makni S, Tounsi A, Jlaiel L, Trigui M, Tounsi S. Effects of Juniperus*phoenicea* hydroalcoholic extract on inflammatory mediators and oxidative stress markers in carrageenan-induced paw oedema in mice. *Biomed Res Int*. 2018;2018:3785487. doi:10.1155/2018/3785487
73. Habib MJ, Akogyeram C, Ahmadi B. Improved dissolution of indomethacin in coprecipitates with phospholipids-I. *Drug Dev Ind Pharm*. 1993;19(4):499–505. doi:10.3109/03639049309063207